Implication of the IL-10/TGFβ Pathway in Age-Associated Neuroinflammation

Undergraduate Honors Research Thesis

Presented in Partial Fulfillment of the Requirements for Graduation
"with Honors Research Distinction in Neuroscience"
in the College of Arts and Sciences of The Ohio State University

by
Starr Jiang

The Ohio State University
April 2020

Project Advisor: Dr. Jonathan Godbout, Department of Neuroscience

Table of Contents

ABSTRACT

Peripheral infections induce prolonged and exaggerated neuroinflammatory responses in the aged brain that result in cognitive impairment, neuropsychiatric complications and ultimately, increased mortality rates. Impaired bidirectional communication between microglia and astrocytes, the primary immune cells of the brain, contributes to a pro-inflammatory microglial phenotype that underlies exacerbated neuroinflammation and sickness behavior. Microglia signal to astrocytes with interleukin (IL)-10; in response, astrocytes regulate microglia with transforming growth factor beta (TGFβ). Aged microglia produce increased levels of both pro- and anti-inflammatory cytokines. However, aged astrocytes exhibit decreased IL-10 receptor (IL-10Rα) expression and are less sensitive to IL-10 signaling. In turn, aged astrocytes produce less TGFβ and are unable to properly attenuate microglial inflammation. We hypothesized that age-associated impairment of this signaling pathway underlies the peripherally induced exaggerated sickness response. Cre/*lox* recombination was used to cross *Aldh1l1-CreER*^{T2} and *Il10ra*$^{flox/flox}$ mouse lines to conditionally knockout astrocytic *Il10ra* upon tamoxifen administration and recapitulate an aged-like phenotype. Concurrently, adeno-associated virus (AAV)-mediated gene therapy was administered directly to astrocytes in the hippocampus of aged mice to augment TGFβ signaling. Mice were administered lipopolysaccharide to induce a peripheral immune response. Social behavioral testing was followed by characterization of glial mRNA via real-time polymerase chain reaction (qPCR). Knockout of *Il10ra* in adult astrocytes impaired astrocytic TGFβ-mediated attenuation of microglia, inducing prolonged and exaggerated neuroinflammation and depressive-like sickness behavior. In aged mice, virally augmenting astrocytic TGFβ ameliorated age-associated exaggeration of inflammatory sickness response to peripheral immune challenge. Together these data implicate this pathway as a potential therapeutic target in resolving cognitive and neuropsychiatric complications stemming from peripheral infections in the elderly.

INTRODUCTION

The consequences of normal aging on the ability of elderly individuals to respond to peripheral infections presents a salient problem for a rapidly aging global population [1, 2, 3]. The efficacy of the body's physiological response to challenges of the peripheral innate immune system declines with age, underscored by alteration of bidirectional communication between the immune system and nervous system [4, 5]. The aged brain maintains a pro-inflammatory signature "primed" to elicit exaggerated and prolonged neuroinflammatory responses upon inductions of peripheral infections such as bacterial and viral infections [6, 7, 8]. The hyperinflammatory response of the central nervous system (CNS) leaves elderly persons more susceptible to myriad adverse long-term outcomes, including neuropsychiatric complications, cognitive impairment, and ultimately, increased mortality rates [4, 9, 10, 11, 12]. Furthermore, age-associated delirium following acute peripheral stimuli is a trademark risk factor for pathologies such as depression, cognitive dysfunction, and neurodegenerative diseases such as Alzheimer's Disease and Parkinson's Disease [13, 14, 15, 16, 17, 18]. Elucidating the mechanisms of breakdown in neuro-immune communication that contribute to exacerbated neuropsychiatric outcomes of peripheral infections is key to better understanding age-associated immunosenescence and mitigating subsequent hyperinflammation in the CNS.

Microglia and astrocytes, glial cell types in the CNS with immune functions, serve a key role in interpreting signaling from the peripheral immune system and inducing a CNS response to peripheral stimuli [19, 20, 21]. Moreover, peripheral immune challenges elicit robust neuroinflammation and pro-inflammatory cytokine-induced sickness behavior, a phenotype recapitulated and well-characterized in rodent models [22, 23, 24, 25, 26, 27]. With age, microglia and astrocytes adopt a more pro-inflammatory, or "primed", profile that lends to more exaggerated neuroinflammatory responses to peripheral immune challenges [28, 29, 30, 31]. Furthermore,

recent findings from our lab demonstrated that microglial repopulation is insufficient to ameliorate this primed state, with the aged brain microenvironment a chief influence on conditioning the microglia to adopt a primed phenotype [6]. Microglial interaction with aged astrocytes serves as an area of interest in elucidating the mechanisms by which the aged brain microenvironment contributes to this conditioning effect. Bidirectional communication between microglia and astrocytes has been implicated as an important factor in maintaining homeostatic function in the central nervous system; in particular, microglia produce anti-inflammatory interleukin (IL)-10 that binds to astrocytic IL-10 receptor and induces astrocytic transforming growth factor beta (TGFβ) signaling which, in turn, attenuates microglial activation and associated neuroinflammation [32, 33, 34, 35, 36]. Aged brains exhibit insensitivity to IL-10 signaling as a result of decreased IL-10 receptor (IL-10Rα) expression [37]. Consequently, through an intracellular signaling cascade, transcription and production of functional TGFβ decreases and impairs astrocytic regulation of microglia, facilitating exaggerated and prolonged neuroinflammation following challenge to the peripheral innate immune system in an *ex vivo* model of glial interaction [32, 38]. Gaining a better understanding of the microglia-astrocyte IL-10/TGFβ signaling pathway and its impact on neuroimmune responses to peripheral infections is crucial to identifying potential targets for treating and preventing age-associated peripherally induced dysfunction.

In this study, we sought to utilize a novel *in vivo* transgenic model of IL-10 receptor dysfunction to characterize the genetic and functional neurobehavioral profile of age-associated IL-10Rα insensitivity. We then aimed to establish a viable gene therapy to mitigate impairment of the IL-10/TGFβ pathway and ameliorate age-associated exaggeration and prolongation of peripherally induced neuroinflammation. Here, we provide novel evidence that astrocytic IL-10 receptor dysfunction is necessary and sufficient for adults to adopt an aged-like phenotype of

exaggerated and prolonged neuroinflammation and sickness behavior following acute peripheral immune challenge. Furthermore, virus-mediated gene therapy augments TGFβ in the aged brain to attenuate age-associated microglial activation and resolve subsequent neuroinflammation and sickness behavior.

METHODS

Mice: All procedures and experiments were performed in accordance with the National Institute of Health Guide for the Care and Use of Laboratory Animals and were approved by The Ohio State University Institutional Animal Care and Use Committee (IACUC). All mice were provided *ad libitum* access to water and standard rodent chow and experienced a standard light/dark cycle. Adult (6-8 weeks old) and aged (16-18 months old) male BALB/c mice were purchased from Charles River (Wilmington, MA) and singly housed to prevent fighting.

*Cre/*lox *recombination and breeding:* Transgenic mice were purchased from The Jackson Laboratory. Male B6;FVB-Tg(Aldh1l1-Cre/ERT2)1Khakh/J mice (Aldh1l1-Cre/ERT2; JAX 029655) were crossed with female B6(SJL)-Il10ra$^{tm1.1Tlg}$/J mice (IL-10Rα^{flox}; JAX 028146). The resulting Cre^{+} offspring were crossed and the offspring genotyped for *Cre* and *Il10ra*$^{WT/flox}$ expression. Finally, *Cre*$^{+}$ *Il10ra*$^{flox/flox}$ mice were crossed with *Cre*$^{-}$ *Il10ra*$^{flox/flox}$ mice to yield a 1:1 ratio of *Cre*$^{+}$:*Cre*$^{-}$ *Il10ra*$^{flox/flox}$ offspring. Litters were separated by sex into cages of 2-5 mice and genotyped for *Cre* expression at post-natal day 21 (P21). All transgenic mice were administered 1.5 mg intraperitoneal (i.p.) tamoxifen in corn oil (10 mg/mL) for five consecutive days three weeks prior to experimentation to induce Cre-Lox recombination in *Cre*$^{+}$ mice.

Peripheral immune challenge with lipopolysaccharide: Adult transgenic mice received a single intraperitoneal (i.p.) injection of saline or 0.50 mg/kg *Escherichia coli* lipopolysaccharide (LPS; serotype 0127:B8; Sigma-Aldrich) as a model of peripheral immune challenge. This LPS dosage was selected because it elicits a pro-inflammatory cytokine response in the brain resulting in a transient sickness response in adult C57BL/6 mice [39]. Similarly, adult and aged BALB/c mice received LPS at a dose of 0.33 mg/kg. This dosage was selected because it elicits a pro-inflammatory cytokine response in the brain resulting in a transient sickness response in adult BALB/c mice without mortality in aged mice [6, 7, 26].

Social exploratory behavior: Social exploration was determined as a measure of sickness behavior as previously described [6]. In brief, test subjects were recorded for baseline social exploratory activity upon introduction of a novel male juvenile mouse to their home cage for 5 min, then injected (t = 0) i.p. with saline or LPS. At t = 4, 8, and 24 h, the social exploration behavioral assay was repeated. Behavior was recorded and the total duration of time the experimental subject engaged in social investigation of the juvenile (e.g. anogenital sniffing, trailing) was determined. At t = 8 h, all nesting material was removed from each cage and replaced with a fresh cotton nestlet. At t = 24 h, the provided fresh nestlet was weighed to determine nesting behavior. Mice were euthanized at either t = 4 or 24 h. Social index for mice euthanized at t = 24 h was calculated as the normalized area under the curve for social interaction (% baseline) v. time post-injection.

Isolation of Percoll-enriched glia: Microglia were isolated from brain homogenates using a Percoll density gradient as previously described [6]. In brief, mice were sacrificed by CO_2 asphyxiation. Brains were collected after decapitation, a 1-mm coronal brain section (Bregma - 1.5 mm) or the

hippocampus harvested and frozen in liquid nitrogen, and the remaining brain tissue homogenized in ice-cold phosphate-buffered saline (PBS) using a 10-mL Potter-Elvehjem tissue grinder (Wheaton). The resulting cell pellet was resuspended in 70% isotonic Percoll (GE Healthcare) and a discontinuous Percoll density gradient was layered and centrifuged at 2,000×*g* for 20 min. Enriched microglia were collected from the interface between the 70% and 50% Percoll layers. Of the cells collected from this interface, >80% of the cells were $CD11b^{+}/CD45^{low}$ microglia. Enriched astrocytes were collected from the interface between the 50% and 35% Percoll layers.

Quantification of gene expression by qPCR: RNA was isolated from coronal brain sections and hippocampi using the Tri-Reagent protocol (Sigma-Aldrich) and from Percoll-enriched microglia using the RNeasy Mini Plus kit (QIAGEN). Reverse transcription was performed using the High Capacity cDNA Reverse Transcription Kit (Applied Biosystems) to produce cDNA. Quantitative real-time (q)-PCR was performed using the TaqMan Gene Expression Assay (Applied Biosystems). In brief, experimental cDNA was amplified using qPCR such that a target gene and reference gene (*Gapdh*) were amplified simultaneously using an oligonucleotide probe with a 5' fluorescent reporter dye (FAM) and 3' non-fluorescent quencher (NFQ). When *Taq* DNA polymerase synthesizes a new strand and reaches the TaqMan probe, the FAM is cleaved from the NFQ and increases the fluorescent intensity proportional to the amount of amplicon synthesized. Fluorescence was determined using a QuantStudio 5 Real-Time PCR System (Applied Biosystems). Data were analyzed using the comparative threshold cycle ($\Delta\Delta C_T$) method and results are expressed as fold change from a control group.

Adeno-associated viral vectors: The following adeno-associated viruses (AAVs) were purchased from Vector BioLabs. The AAV5-GFAP(0.7)-eGFP (AAV-GFP) consists of an AAV5 capsid with AAV2 ITR. The virus expresses enhanced green fluorescent protein (eGFP) under a shortened 0.7-kB GFAP promoter. The AAV5-GFAP(0.7)-mTGFb1(C223S/C225S)-IRES-GFP (AAV-TGFβ) consists of an AAV5 capsid with AAV2 ITR. The virus expresses eGFP alongside mouse *Tgfb1* with two point mutations (C223S and C225S; RefSeq# NM_011577) under the same GFAP(0.7) promoter. These mutations render the produced TGFβ1 protein biologically active.

Intra-cerebral hippocampal injection of AAV vectors: Adult and aged male BALB/c mice were anesthetized with 5% isoflurane induction, placed in the stereotaxic frame (David Kopf Instruments), and maintained at 1.0-1.5% isoflurane during surgery. The skull was exposed and coordinates for craniotomy were precisely located by a motorized stereotactic instrument (David Kopf Instruments). The following coordinates were used for bilateral hippocampal injections: -1.82 mm AP, ±1.57 ML, and +1.85 DV. A small hole was drilled through the skull above these coordinates and a 10-μL Hamilton syringe slowly lowered into the brain. AAV vectors were injected at 10^{10} GC per 2-μL injection per hemisphere at a rate of 0.4 μL/min. The needle was left in place for an additional 1 min and then slowly withdrawn. Wounds were closed with surgical staples and mice returned to their home cages for recovery.

Detection of hippocampal TGFβ protein: Hippocampal tissue was sonicated in 300 μL Tissue Protein Extraction Reagent (Thermo) supplemented 1:100 with proteinase inhibitor. Hippocampal TGFβ protein was then detected using the Mouse TGF Beta 1 ELISA Kit PicoKine™ (Boster) according to manufacturer's protocols. Optical density absorbance was measured at 450 nm on a

SpectraMax 190 microplate reader (Molecular Devices). Protein concentrations were calculated based on absorbance readings of a serial dilution of TGFβ1 protein of known concentration.

Statistical analysis: Statistical analysis was performed using GraphPad Prism software (San Diego, CA). To determine significant main effects and interactions between variables, two- or three-way analysis of variance (ANOVA) was performed. Comparison between groups was performed using Student's *t*-test and Bonferroni's correction for multiple comparisons. A value of $P < 0.05$ was considered statistically significant. All data are presented as mean ± standard error of the mean (SEM).

RESULTS

Astrocyte-specific *Il10ra* knockout impairs propagation of a functional TGFβ response. Previous work from our lab and others have implicated impairment of IL-10/TGFβ signaling between microglia and astrocytes as a critical contributor to age-associated prolonged and exaggerated neuroinflammation stemming from unresolved microglial activation [32, 35, 37]. Accordingly, we sought to further characterize mechanisms of this pathway and potential therapeutic methods to attenuate detrimental neuroinflammation. Our first objective was to develop and maintain a transgenic mouse breeding colony to produce a Cre^{+} (and Cre^{-} control) $Il10ra^{f/ox/flox}$ line allowing inducible *Il10ra* knockout as an *in vivo* murine model of age-associated IL-10 receptor insensitivity [37]. Cre^{+} and *Il10ra* knockout are interchangeably synonymous in this study for the Cre^{+} $Il10ra^{flox/flox}$ genotype. Tamoxifen was administered to induce Cre/*lox* recombination, excising floxed Exon 3 of the IL-10 receptor and rendering it dysfunctional (Fig. 1A). Reporter strains were imaged with Evos fluorescent microscopy, where robust expression of

tdTomato fluorescent protein reflected viable and effective induction of Cre/*lox* recombination (Fig. 1B).

Cre^- and Cre^+ test subjects were injected (i.p.) with LPS or saline and sacrificed 4 h and 24 h post-injection. Quantification of *Il10ra* expression via qPCR revealed distinct genetic profiles between brain slice mRNA and astrocyte mRNA at t = 24 h. Fold change of *Il10ra* was relatively uniform across all groups in the whole brain, with no significant differences, whereas a main effect of LPS ($F(1, 16) = 5.25$, $P < 0.05$) and trend by knockout ($F(1, 16) = 3.278$, $P < 0.09$) existed in the astrocyte profile (Fig. 1C). Post hoc analysis revealed that LPS-treated Cre^+ subjects express lower *Il10ra* compared to both genotype-matched saline controls ($t(16) = 3.34$, $P < 0.01$) and treatment-matched Cre^- controls ($t(16) = 3.00$, $P < 0.05$), reflecting astrocyte-specific knockout of *Il10ra* following peripheral immune challenge in Cre^+ $Il10ra^{flox/flox}$ mice. To assess the downstream effects of *Il10ra* knockout on IL-10/TGFβ signaling, we then quantified astrocytic *Tgfb1* expression with qPCR, finding a non-significant trend of decreased *Tgfb1* in LPS-treated mice at t = 4 h, followed by a main effect of knockout ($F(1, 16) = 6.81$, $P < 0.05$) and a trend by LPS ($F(1, 16) = 3.19$, $P < 0.10$) on *Tgfb1* expression at t = 24 h (Fig. 1D). Moreover, post hoc analysis revealed lower expression of *Tgfb1* in LPS-treated Cre^+ mice compared to both genotype-matched saline controls ($t(16) = 3.24$, $P < 0.05$) and treatment-matched Cre- controls ($t(16) = 3.83$, $P < 0.01$). Taken together, the tamoxifen induction of the Cre^+ $Il10ra^{flox/flox}$ genotype functionally knocks out *Il10ra*, impairing astrocytic production of TGFβ following the acute phase of LPS-induced peripheral immune challenge.

Impairment of TGFβ-mediated attenuation facilitates acute microglial activation and exaggerated sickness behavior 4 hours after peripheral immune challenge. With a viable *in*

vivo transgenic murine model (Fig. 2A), we sought to further elucidate genetic and functional consequences of astrocytic *Il10ra* knockout and impaired TGFβ production on the inflammatory profile of the brain microenvironment in the acute phase of activation following LPS injection [7, 20, 24, 26, 27]. Tamoxifen-induced Cre^+ and Cre^- $Il10ra^{flox/flox}$ mice were given i.p. LPS or saline injections and sacrificed at t = 4 h (Fig. 2B). qPCR analysis of Percoll-enriched microglia revealed main effects of knockout ($F(1, 11) = 6.18$, $P < 0.05$) and LPS ($F(1, 11) = 189.40$, $P < 0.0001$), as well as an interaction effect between knockout and LPS ($F(1, 11) = 7.10$, $P < 0.05$), on expression of pro-inflammatory cytokine *Il1b* expressed as fold change. Additional post hoc analysis showed a significant increase compared to genotype-matched saline controls ($t(11) = 11.19$, $P < 0.0001$) and treatment-matched Cre^- controls ($t(11) = 3.79$, $P < 0.01$) for LPS-injected Cre^+ $Il10ra^{flox/flox}$ mice (Fig. 2C). There was a main effect of LPS on *Tnf* expression ($F(1, 12) = 41.60$, $P < 0.0001$). Accordingly, *Tnf* expression was significantly lower compared to genotype-matched saline controls for both Cre^- ($t(12) = 5.35$, $P < 0.001$) and Cre^+ ($t(12) = 3.78$, $P < 0.01$) LPS-injected mice. Gene analysis of representative brain slices via qPCR revealed a main effect of LPS ($F(1, 15) = 4.73$, $P < 0.05$) and a trend of knockout ($F(1, 15) = 3.38$, $P < 0.09$) on expression of reactive astrocyte marker *Gfap* (Fig. 2D). Social exploratory behavior was recorded and analyzed at t = 0 h and 4 h to assess functional consequences of *Il10ra* knockout (Fig. 2E). There were significant main effects of LPS ($F(1, 67) = 41.88$, $P < 0.0001$) and knockout ($F(1, 67) = 8.04$, $P < 0.01$) on social interaction at t = 4 h (Fig. 2F). Notably, social interaction of LPS-injected Cre^+ mice was significantly decreased compared to genotype-matched saline controls ($t(67) = 5.42$, $P < 0.0001$) and treatment-matched Cre^- controls ($t(67) = 2.91$, $P < 0.01$). Comprehensive analysis at t = 4 h following LPS injection reveals an acute inflammatory signature characterized by glial activation

(Fig. 2C, D) and social withdrawal (Fig. 2F) that was further exacerbated by astrocytic *Il10ra* knockout.

Prolonged microglial neuroinflammation persists in an IL-10Rα$^{A\text{-}cKO}$ murine model 24 hours post-peripheral immune challenge. Peripheral innate immune challenge induces neuroinflammation and sickness response that is both exaggerated and prolonged in the aged brain [7, 22, 24, 27]. Thus, we aimed to characterize the consequences of *Il10ra* knockout on resolution of peripherally induced neuroinflammation over time by analyzing the genetic profile of *Cre*$^{-}$ and *Cre*$^{+}$ *Il10ra*$^{flox/flox}$ 24 h after i.p. injection of saline or LPS (Fig. 3A, B). There were significant main effects of LPS ($F(1, 31) = 151.60$, $P < 0.0001$) and knockout ($F(1, 31) = 27.91$, $P < 0.0001$), as well as a significant interaction effect between LPS and knockout ($F(1, 31) = 24.43$, $P < 0.0001$), on microglial *Il1b* expression at $t = 24$ h (Fig. 3C). Further post hoc analysis revealed a significant increase in *Il1b* fold change in LPS-injected Cre^{+} mice compared to genotype-matched saline controls ($t(31) = 12.02$, $P < 0.0001$) and treatment-matched Cre^{-} controls ($t(31) = 7.12$, $P < 0.0001$). Similarly, there were significant main effects of LPS ($F(1, 31) = 54.23$, $P < 0.0001$) and knockout ($F(1, 31) = 6.09$, $P < 0.05$), as well as an interaction effect between LPS and knockout ($F(1, 31) = 7.43$, $P < 0.05$), on microglial *Tnf* expression at $t = 24$ h (Fig. 3C). Post hoc analysis revealed a significant increase in *Tnf* fold change in LPS-injected Cre^{+} mice compared to genotype-matched saline controls ($t(31) = 7.03$, $P < 0.0001$) and treatment-matched Cre^{-} controls ($t(31) = 3.62$, $P < 0.01$). qPCR analysis of brain slice mRNA was conducted to profile the broader brain microenvironment. There was a main effect of LPS on *Gfap* expression ($F(1, 32) = 12.56$, $P < 0.01$). Moreover, LPS-injected Cre^{+} mice had lower *Gfap* compared to genotype-matched saline controls ($t(32) = 3.97$, $P < 0.001$) and a trend of decrease compared to treatment-matched Cre^{-}

controls (t(32) = 2.34, $P < 0.06$) (Fig. 3D). Reactive astrocyte marker *Vim* was also quantified via qPCR and expressed as fold change. There were main effects of LPS (F(1, 16) = 9.56, $P < 0.01$) and knockout (F(1, 16) = 5.68, $P < 0.05$), as well as an interaction effect between LPS and knockout (F(1, 16) = 6.75, $P < 0.05$), on *Vim* expression at t = 24 h (Fig. 3D). Post hoc analysis further identified significant increase in *Vim* expression in LPS-injected Cre^+ mice compared to genotype-matched saline controls (t(16) = 4.02, $P < 0.01$) and treatment-matched Cre^- controls (t(16) = 3.52, $P < 0.01$). These data together reveal an prolonged inflammatory profile of glial activation at t = 24 h that reflects an inability of Cre^+ $Il10ra^{flox/flox}$ knockout mice to properly resolve microglial activation and attenuate exaggerated neuroinflammation.

Unresolved *Il10ra* knockout-mediated microglial activation and neuroinflammation underlies prolonged social withdrawal sickness behavior. Peripheral challenge of the aged innate immune system elicits exaggerated and prolonged neuroinflammation that is associated with prolonged depressive-like sickness behavior [7, 39]. Our study assessed whether transgenic astrocytic *Il10ra* knockout recapitulated age-associated prolonged sickness behavior mediated by IL-10Rα insensitivity [37]. Body masses of saline- or LPS-injected Cre^- or Cre^+ mice were recorded at t = 0 h and t = 24 h to assess change in body weight. There were main effects of LPS (F(1, 32) = 161.30, $P < 0.0001$) and knockout (F(1, 32) = 6.45, $P < 0.05$), as well as an interaction effect between LPS and knockout (F(1, 32) = 10.89, $P < 0.01$), on change in body mass (Fig. 4A). Furthermore, LPS-injected Cre^+ mice displayed greater magnitude of weight loss compared to genotype-matched saline controls (t(32) = 11.32, $P < 0.0001$) and treatment-matched Cre^- controls (t(32) = 4.13, $P < 0.001$). This corresponded with food consumption measurements, where there were main effects of LPS (F(1, 32) = 116.40, $P < 0.0001$) and knockout (F(1, 32) = 5.94, $P < 0.05$),

as well as an interaction effect between LPS and knockout ($F(1, 32) = 4.81$, $P < 0.05$, Fig. 4B). Post hoc analysis revealed lower food consumption in LPS-injected Cre^+ mice compared to genotype-matched saline controls ($t(32) = 9.18$, $P < 0.0001$) and treatment-matched Cre^- controls ($t(32) = 3.27$, $P < 0.01$). There were also main effects of LPS ($F(1, 32) = 10.02$, $P < 0.01$) and knockout ($F(1, 32) = 5.35$, $P < 0.05$), as well as an interaction effect between LPS and knockout ($F(1, 32) = 4.88$, $P < 0.05$), on nesting behavior (Fig. 4C). LPS-injected Cre^+ mice utilized less nestlet material than genotype-matched saline controls ($t(32) = 3.80$, $P < 0.01$) and treatment-matched Cre^- controls ($t(32) = 3.20$, $P < 0.01$). Social index was analyzed as previously described, eliciting main effects of LPS ($F(1, 32) = 4.82$, $P < 0.05$) and knockout ($F(1, 32)$, $P < 0.01$, Fig. 4D). Knockout of *Il10ra* exacerbated sickness response, as LPS-injected Cre^+ mice had a significantly lower social index than treatment-matched Cre^- mice ($t(32) = 3.03$, $P < 0.01$). Social exploratory behavior was also expressed in a time-course format (Fig. 4E), where there were main effects of LPS and knockout at $t = 4$ h ($F(1, 67) = 41.88$, $P < 0.0001$ and $F(1, 67) = 8.04$, $P < 0.01$, respectively) and $t = 8$ h ($F(1, 32) = 6.11$, $P < 0.05$ and $F(1, 32) = 6.27$, $P < 0.05$, respectively), with a main effect of knockout at $t = 24$ h ($F(1, 32) = 6.91$, $P < 0.05$), on social interaction. LPS-injected Cre^+ mice exhibited less social interaction compared to genotype-matched saline controls and treatment-matched Cre^- controls at both $t = 4$ h ($t(67) = 5.42$, $P < 0.0001$ and $t(67) = 2.91$, $P < 0.01$, respectively) and $t = 8$ h ($t(32) = 2.51$, $P < 0.05$ and $t(32) = 2.53$, $P < 0.05$, respectively). Overall, *Il10ra* knockout exacerbates an LPS-induced sickness response and mediates an inability to resolve prolonged and exaggerated microglial activation, underlying a poor recovery time-course in social exploratory behavior.

Viral Tgfb1 administration circumvents IL-10 receptor insensitivity and augments TGFβ expression in aged mice. To complement elucidation of the genetic and behavioral consequences of IL-10Rα knockout, we sought to identify a potential therapeutic approach to IL-10/TGFβ-mediated breakdown in astrocytic attenuation of microglial neuroinflammation. We utilized adeno-associated virus (AAV) mediated gene therapy with hybrid serotype AAV2/5 to deliver mutant *Tgfb1* to hippocampal astrocytes with high transduction efficiency [40]. Adult (6-8 wks) and aged (16-18 mos.) male BALB/c mice received bilateral intra-cerebral injections of AAV-GFP (control) or AAV-TGFβ and allowed three weeks of virus transduction, followed by i.p. injection of saline or LPS at t = 0 h (Fig. 5A, B). Social exploratory behavior was assessed at t = 0, 4, 8, and 24 h, and subjects were sacrificed and cells harvested for gene analysis at t = 24 h. Fluorescent histological imaging of immunostained coronal brain slices revealed robust expression of green fluorescent protein (GFP) in both adult and aged mice, reflecting efficient, astrocyte-specific transduction of the AAVs (Fig. 5C). Due to COVID-19 research shutdowns, sample sizes of the AAV experiments were insufficient for conclusive statistical analyses, as determined by a power analysis. Percoll-enriched astrocytes were processed for mRNA isolation, reverse transcription, and qPCR analysis. There were non-significant differences in *Il10ra* expression across AAV-GFP and AAV-TGFβ groups, indicating the virus circumvented the *Il10ra* insensitivity of aged mice (Fig. 5D) to augment TGFβ. Augmentation was evident at both the genetic and functional level of TGFβ expression. There was a robust increase in *Tgfb1* mRNA fold change for all AAV-TGFβ groups compared to age- and vector-matched AAV-GFP controls (Fig. 5E). An ELISA assay of functional TGFβ1 protein yielded corresponding increases in AAV-TGFβ mice compared to treatment-matched AAV-GFP controls (Fig. 5F). Viral administration of AAV-TGFβ augments expression of *Tgfb1* mRNA and TGFβ1 protein in an *Il10ra*-independent manner.

Augmentation of TGFβ ameliorates microglial activation and subsequent age-associated sickness behavior. Genetic and behavioral assays were conducted and analyzed to assess functional outcomes of TGFβ augmentation. As previously described (Fig. 5A, B, C), AAV-GFP or AAV-TGFβ were administered to adult and aged male BALB/c mice via intra-cerebral injection, followed by i.p. injection of saline or LPS. Microglial *Il1b* and *Tnf* were quantified with qPCR to characterize the pro-inflammatory signature (Fig. 6A). Both genes were increased in LPS-injected mice compared to age- and vector-matched saline controls. Additionally, pro-inflammatory signatures were heavily exacerbated in aged mice administered AAV-GFP control virus, while AAV-TGFβ administration ameliorated exaggerated inflammation and restored *Il1b* and *Tnf* expression levels to adult baselines. qPCR analysis of hippocampal tissue, where the virus was injected and concentrated, these trends were recapitulated in *Il1b* expression, with aged AAV-GFP mice expressing robust increase in fold change that is rescued with AAV-TGFβ administration (Fig. 6B). Behavioral assays revealed a corresponding interaction. Aged mice administered AAV-GFP and challenged with LPS exhibited the most weight loss, a trend reversed by administration of AAV-TGFβ (Fig. 6C). Social index analysis revealed a markedly low level of social interaction in aged LPS-injected AAV-GFP mice that was rescued with AAV-TGFβ administration (Fig. 6D). A 24h time course of social exploratory behavior showed acute decrease in social interaction of aged LPS-injected AAV-GFP mice followed by an inability to recover to baseline levels over time (Fig. 6E). Administration of AAV-TGFβ to age- and LPS-matched mice elicited less exaggerated social sickness behavior at t = 4 h and improved recovery outcomes over time. The hyper-inflammatory genetic signature of aged mice challenged with LPS underlie exaggerated sickness behavior that is ameliorated with AAV-TGFβ-mediated gene therapy.

DISCUSSION

This study sought to characterize the IL-10/TGFβ signaling pathway between microglia and astrocytes and its implications in age-associated neuro-immune dysfunction. Our primary objectives were to determine whether IL-10Rα dysfunction is necessary and sufficient to induce prolonged and exaggerated microglial neuroinflammation and sickness behavior, and whether viral augmentation of TGFβ is sufficient to mitigate this dysfunction and attenuate the age-associated breakdowns in neuro-immune response to peripheral immune challenges.

We established the viability of a transgenic murine *Il10ra* knockout model to recapitulate aged-like deficits in *Il10ra* expression. Cre/*lox* site-specific recombination enabled the development of an *Aldh1l1-Cre*$^{ERT2+}$ *Il10ra*$^{flox/flox}$ line that induced *Il10ra* knockout upon tamoxifen administration (Fig. 1A). The selection of *Aldh1l1-Cre* recombinase leveraged *Aldh1l1* as an established pan-astrocyte marker to induce highly efficient and astrocyte-specific knockout [41, 42]. Indeed, non-significant differences in *Il10ra* expression across groups in whole brain tissue contrasted with a significant decrease in *Il10ra* expression in an astrocyte assay of LPS-injected Cre^{+} mice (Fig. 1C). This pointed to an astrocyte-specific induction of *Il10ra* knockout, although there was not a significant main effect of knockout. This could be mitigated with an alternative quantification method, such as quantifying co-localization of *Sox9/pStat3* via histological immunochemistry analysis or quantifying *Il10ra* expression of GLAST^{+} astrocytes via flow cytometry, as qPCR quantification of *Il10ra* presents difficulty due to a low baseline expression of *Il10ra* from cortical astrocytes. Previous work from our lab has shown that astrocyte cytokine induction is delayed in comparison to microglial proinflammatory cytokine expression [20]. Moreover, TGFβ expression does not reach its peak until t = 12 h following LPS challenge. Indeed, following *Il10ra* dysfunction, astrocytic *Tgfb1* expression was undifferentiated across groups at t = 4 h, but was significantly lower for Cre^{+} knockout mice compared to treatment-matched Cre^{-}

mice at *t* = 24 h (Fig. 1D). *Tgfb1* expression emulated the previously established sequential timeframe, increasing after the acute inflammation phase at *t* = 4 h following peripheral immune challenge to resolve microglial activation, with the exception of *Il10ra* knockout mice, which displayed impaired TGFβ signaling.

Transgenic knockout of *Il10ra* effectively disrupted homeostatic IL-10/TGFβ signaling and impaired TGFβ-mediated anti-inflammatory response to microglial activation following the acute stage of LPS immune challenge. Thus, we sought to further elucidate the neurobehavioral profile at various timepoints encompassing the acute and prolonged phases of lipopolysaccharide-induced neuroinflammation [34, 37]. We began with the *t* = 4 h timepoint, representative of the acute phase. A robust increase in microglial expression of pro-inflammatory cytokine *Il1b* from saline controls to LPS-injected mice was further exacerbated by *Il10ra* knockout, emulating aged-like exaggeration of microglial inflammation with *Il10ra* dysfunction (Fig. 2C). A main effect of LPS was also observed in *Tnf* expression but did not follow the same pattern of knockout-mediated exacerbation. This points to the possibility of an *Il1b*-mediated acute neuroinflammatory response to IL-10/TGFβ signaling impairment. A main effect of LPS on expression of *Gfap*, a marker of astrocyte reactivity [43], accompanied by a marked upregulation of *Gfap* in LPS-injected knockout subjects signified a shift toward a reactive astrocyte profile (Fig. 2D). Notably, previous work reported absence of GFAP immunoreactivity following LPS administration [20], indicating this increase in astrocyte reactivity is knockout-mediated. These genetic profiles aligned with concomitant social exploratory behavior testing, which revealed a significant decrease in social interaction at the acute timepoint following LPS administration, which was further exacerbated by *Il10ra* knockout (Fig. 2F). Taken together, these gene and behavioral data reflect an acute neurobehavioral response of *Il10ra* knockout mice to peripheral immune challenge at *t* = 4 h.

Previous studies have reported the transient nature of the acute LPS response, followed by rapid recovery from sickness 24-48 h post-injection [7, 20, 26]. However, age-associated deficits result in a prolonged period of neuroinflammation and impaired resolution of microglial activation [4, 22, 27]. Accordingly, we conducted gene and behavioral assays at t = 24 h following LPS injection to study the recovery profile of *Il10ra* knockout mice. We hypothesized that they would recapitulate an aged-like phenotype of persistent microglial neuroinflammation and prolonged sickness behavior. Indeed, microglial expression of pro-inflammatory cytokines *Il1b* and *Tnf* revealed similar profiles of prolonged increase at t = 24 h in LPS-injected groups, an escalation significantly further exacerbated by Cre^+ *Il10ra* knockout (Fig. 3C). Notably, *Tnf* expression in the LPS-injected Cre^+ group was significantly increased compared to treatment-matched Cre- controls ($P < 0.01$), an effect that was not present at the t = 4 h timepoint. This points to a delayed interaction effect between LPS and knockout in exacerbating *Tnf* contribution to neuroinflammation. Moreover, fold change levels were lower across the LPS groups at t = 24 h compared to the t = 4 h, reflecting an overall profile of recovery; however, as expected, this recovery is impaired in the Cre^+ knockout group in the form of prolonged microglial neuroinflammation. Gene analysis of representative whole brain tissue revealed increased *Gfap* and *Vim* expression with concomitant LPS injection and *Il10ra* knockout. Previous work from our lab has provided evidence that GFAP immunoreactivity of astrocytes in the hippocampus is unaffected after LPS challenge [20]. While reactive astrogliosis mediated by intermediate filaments such as GFAP and vimentin serves important neuroprotective roles in response to acute stressors such as CNS injury and trauma, the same astrocytic reactivity has been associated with aging and neuroinflammatory pathologies, making it a marker of interest [43, 44, 45, 46, 47, 48, 49]. Furthermore, the degree of GFAP immunoreactivity in the aged brain has been positively

linked with extent of cognitive impairment [50]. Significantly lower *Gfap* and *Vim* expression in LPS-injected Cre^+ knockout mice compared to matched saline and Cre^- controls provided evidence that interaction between LPS and *Il10ra* knockout induces aged-like hyperreactivity in astrocytes (Fig. 3D). Taken together, these genetic data characterize a persistent hyperinflammatory signature at t = 24 h following peripheral immune challenge, mediated by impaired resolution of microglial activation.

We then assessed social exploratory behavior, weight loss, nesting behavior, and food consumption for evidence of neuroinflammation-associated sickness behavior emulating an aged-like phenotype. Here, we provide evidence of exacerbated behavioral deficits in LPS-injected Cre^+ *Il10ra* knockout mice indicative of neuroinflammation-induced prolonged sickness behavior. There were significant main effects of LPS and knockout, as well as interaction effects between the two variables for weight change, food consumption, and nesting behavior, for each of the behavioral assays conducted (Fig. 4). Furthermore, LPS-injected *Il10ra* knockout mice exhibited significantly more weight loss, less food consumption, less nesting behavior, and less social interaction expressed as social index compared to their LPS-injected Cre^- counterparts. This robust difference by genotype underscores an *Il10ra* knockout-mediated exacerbation of sickness behavior that recapitulates age-associated prolonged depressive-like and social withdrawal behavior. Closer examination of a full 24 h time-course of social behavioral response to LPS immune challenge provides a visual representation of exaggerated sickness behavior at the acute time point (t = 4 h) followed by an impaired and prolonged recovery through the 8 and 24 h timepoints in LPS-injected Cre^+ *Il10ra* knockouts (Fig. 4E). The persistent exacerbation of microglial neuroinflammation at t = 24 h underlies *Il10ra* dysfunction-mediated prolongation of sickness behavior through t = 24 h following peripheral immune challenge.

Following the recapitulation of an aged-like phenotype of prolonged and exaggerated neuroinflammation underlying sickness behavior in an *in vivo Il10ra* knockout model, we sought to identify a viable targeted gene therapy to mitigate age-associated *Il10ra* dysfunction. We employed adeno-associated virus (AAV) to deliver gene therapy to astrocytes in the hippocampus, achieving high efficiency and specificity with the hybrid serotype AAV2/5 and a GFAP(0.7) promoter [40]. The control AAV-GFP virus (AAV2/5-GFAP(0.7)-eGFP) exclusively expressed enhanced green fluorescent protein (eGFP), whereas the experimental AAV-TGFβ virus (AAV2/5-GFAP(0.7)-mTGFb1(C223S/C225S)-IRES-GFP) expressed eGFP as well as mutant *Tgfb1* that yielded biologically active TGFβ1 (Fig. 5A, C). The AAV-mediated gene therapy transduced *Tgfb1* mRNA and induced production of functional TGFβ1 protein in an *Il10ra*-independent manner (Fig. 5D). Increase of *Tgfb1* and TGFβ1 was robust and present across all age and LPS treatment groups administered AAV-TGFβ, demonstrating substantial ubiquitous hippocampal augmentation of TGFβ with AAV-mediated gene therapy (Fig. 5E, F).

We hypothesized TGFβ augmentation was sufficient to mitigate consequences of age-associated *Il10ra* dysfunction and attenuate prolonged and exaggerated neurobehavioral signatures. Indeed, microglial expression of *Il1b* and *Tnf* were heightened with LPS and exacerbated by age when administered the AAV-GFP vector. However, administration of AAV-TGFβ ameliorated this age-associated hyperinflammation, with expression levels emulating adult-like profiles (Fig. 6A). Analysis of the microenvironment of the hippocampus produced a similar profile, with significantly heightened *Il1b* expression in LPS-injected aged AAV-GFP mice attenuated in matched AAV-TGFβ mice (Fig. 6B). Weight loss and social index assays followed this AAV-mediated exacerbation/attenuation contrast (Fig. 6C, D). A 24 h time-course showed acute social exploratory behavioral deficits in the aged AAV-GFP LPS group with an ensuing

impaired recovery of baseline social interaction (Fig. 6E). Administration of AAV-TGFβ in an age- and LPS-matched group yielded markedly less acute sickness behavior at $t = 4$ h and improved recovery through 24 h. Taken together, we provide novel evidence that the augmentation of TGFβ via AAV-mediated gene therapy mitigates age-associated prolongation and exaggeration of microglial neuroinflammation and resolves exacerbation of sickness behavior.

As previously discussed, future investigation will supplement our study of AAV2/5-mediated gene therapy with additional cohorts to increase *n* and achieve sufficient sample sizes as dictated by a power analysis, upon reinstatement of laboratory research following COVID-19 closures. Future studies will also seek to elucidate the intracellular and downstream signaling mechanisms that contribute to age-associated dysfunction and corresponding mitigation of the IL-10/TGFβ pathway. Single-cell RNA sequencing (scRNA-seq) will aim to reveal genes and canonical pathways of interest in a study of the 4 h and 24 h timepoints of LPS immune challenge of aged mice, as well as distributions and characteristics of distinct glial populations [51]. The vast array of data produced by such experimentation will provide an in-depth, multi-layered analysis of genes and cell types implicated in the IL-10/TGFβ pathway and age-associated alteration of neuro-immune functions. We will also be conducting immunohistochemistry for quantifiable histological analysis of glial interactions in a transgenic *Il10ra* knockout model and AAV-TGFβ gene therapy model. Optimizing longevity and increasing health spans for an aging population begins with mitigating development of physiological impairment to preserve healthy function [52]. We aim to comprehensively characterize the IL-10/ TGFβ pathway and its viability as a potential therapeutic target for resolving age-associated neuroimmune dysfunction in elderly individuals.

CONCLUSION

In this study we provided novel evidence that *Il10ra* dysfunction is necessary and sufficient to induce an aged-like phenotype of prolonged and exaggerated neuroinflammation with sickness behavioral consequences. Knockout of astrocytic *Il10ra* impairs TGFβ-mediated regulation of microglia, facilitating an exaggerated inflammatory neurobehavioral signature during the acute phase and persistent impairment of neuroinflammation attenuation through 24 hours following peripheral immune challenge. Moreover, the age-associated hyperinflammatory profile is attenuated with adeno associated virus-mediated gene therapy delivery of mutant *Tgfb1* to augment TGFβ signaling. Genetic and behavioral consequences of age-associated exacerbation of neuroinflammation resulting from *Il10ra* dysfunction are mitigated by AAV-TGFβ-mediated resolution of microglial activation. Taken together, these data implicate the IL-10/TGFβ pathway as a key mediator of age-associated neuroimmune dysfunction and potential therapeutic target for improving longitudinal clinical outcomes of acute peripheral infections for a rapidly growing geriatric population.

FIGURES

Figure 1

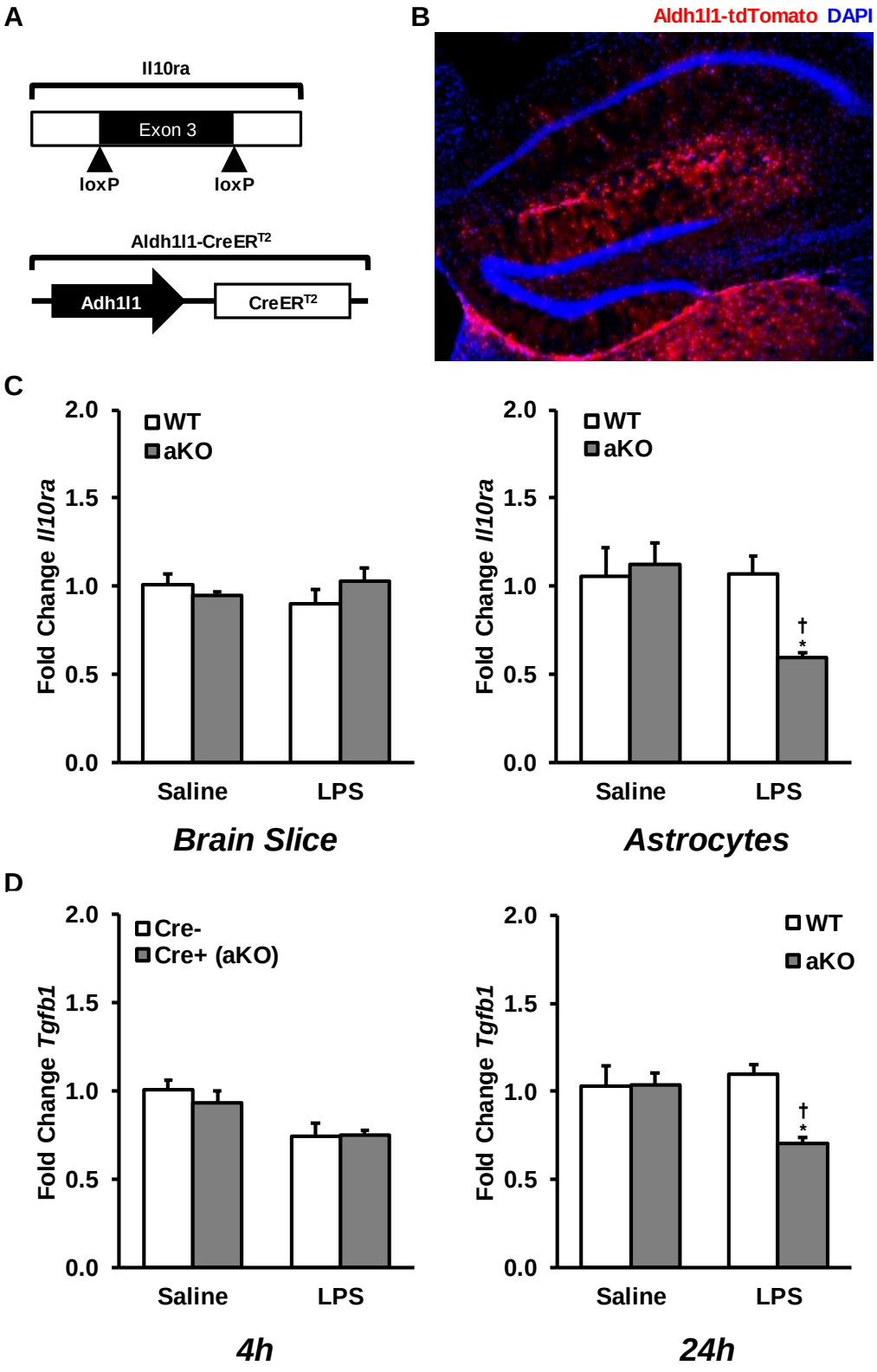

Figure 2

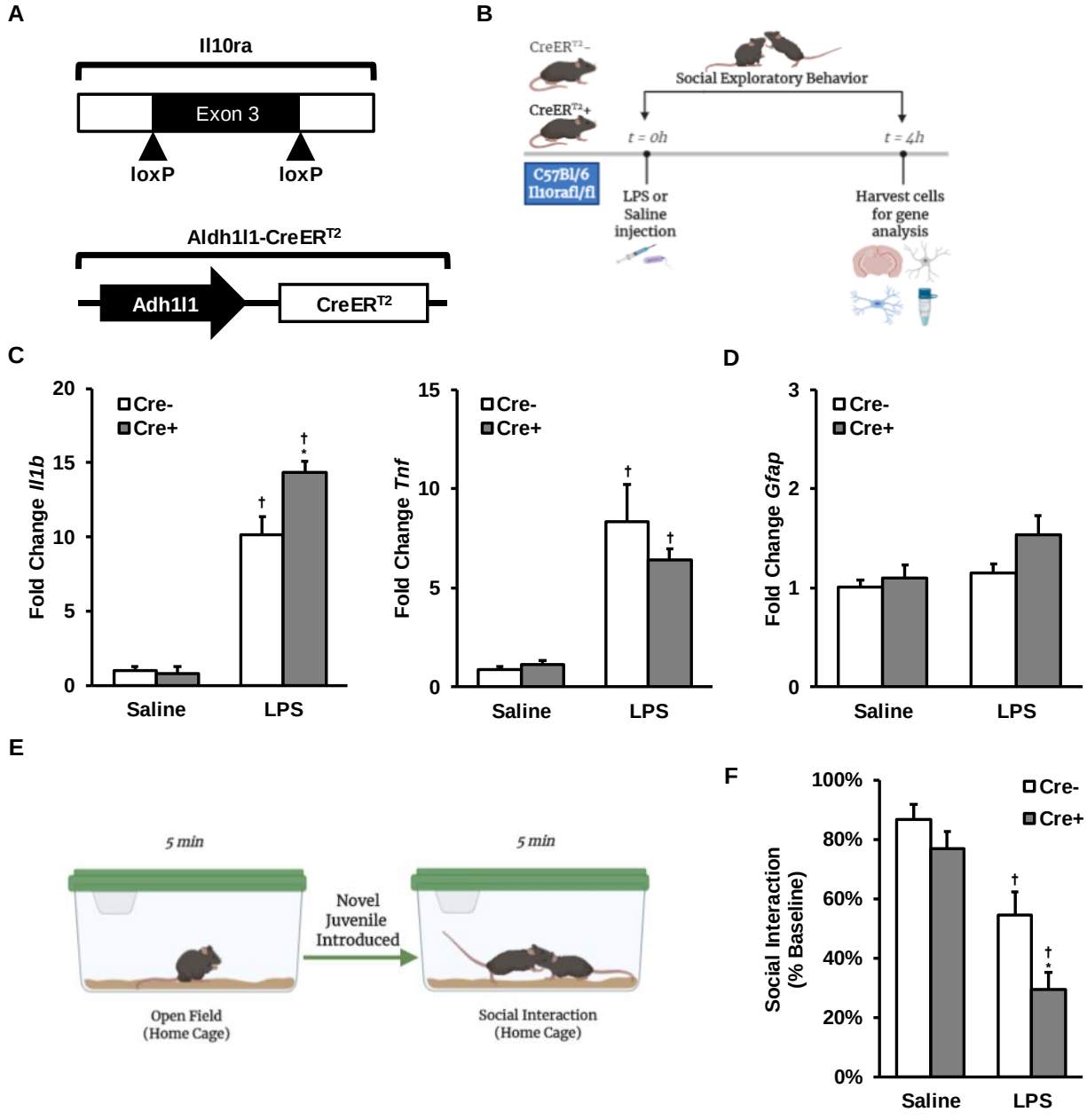
A
Il10ra
Exon 3
loxP
loxP
Aldh1l1-CreER^{T2}
Adh1l1
CreER^{T2}
B
CreER^{T2}-
CreER^{T2}+
Social Exploratory Behavior
t = 0h
t = 4h
C57Bl/6 Il10rafl/fl
LPS or Saline injection
Harvest cells for gene analysis
C
Fold Change Il1b
Cre-
Cre+
Saline
LPS
Fold Change Tnf
D
Fold Change Gfap
E
5 min
5 min
Novel Juvenile Introduced
Open Field (Home Cage)
Social Interaction (Home Cage)
F
Social Interaction (% Baseline)

Figure 3

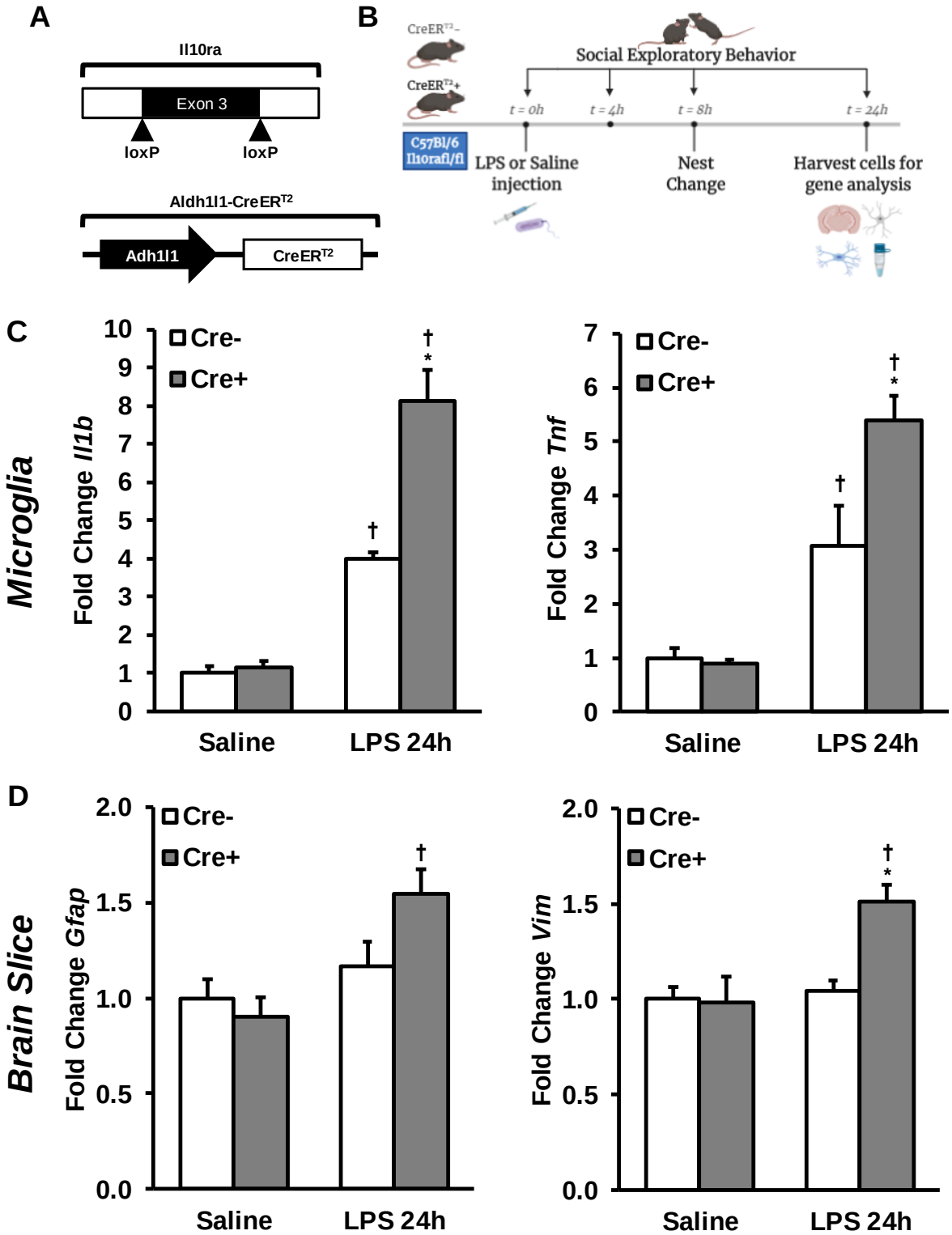
A
Il10ra
Exon 3
loxP
loxP
Aldh1l1-CreER^{T2}
Adh1l1
CreER^{T2}
B
CreER^{T2}-
CreER^{T2}+
C57Bl/6 Il1orafl/fl
Social Exploratory Behavior
t = 0h
t = 4h
t = 8h
t = 24h
LPS or Saline injection
Nest Change
Harvest cells for gene analysis
C
Microglia
Fold Change Il1b
Cre-
Cre+
Saline
LPS 24h
Fold Change Tnf
D
Brain Slice
Fold Change Gfap
Fold Change Vim

Figure 4

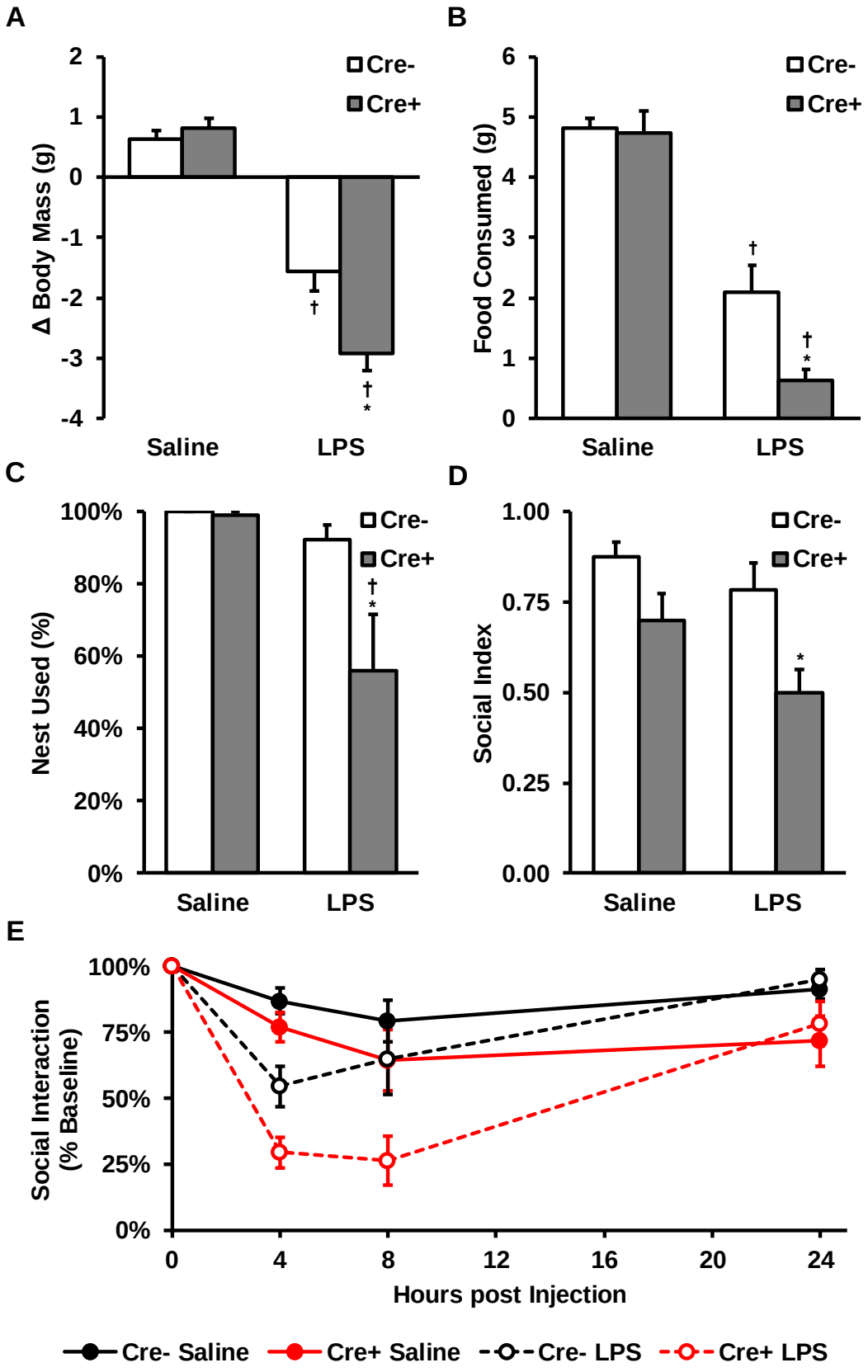
A
Δ Body Mass (g)
2
1
0
-1
-2
-3
-4
Cre-
Cre+
†
†
*
Saline
LPS
B
Food Consumed (g)
6
5
4
3
2
1
0
Cre-
Cre+
†
†
*
Saline
LPS
C
Nest Used (%)
100%
80%
60%
40%
20%
0%
Cre-
Cre+
†
*
Saline
LPS
D
Social Index
1.00
0.75
0.50
0.25
0.00
Cre-
Cre+
*
Saline
LPS
E
Social Interaction (% Baseline)
100%
75%
50%
25%
0%
0
4
8
12
16
20
24
Hours post Injection
Cre- Saline
Cre+ Saline
Cre- LPS
Cre+ LPS

Figure 5

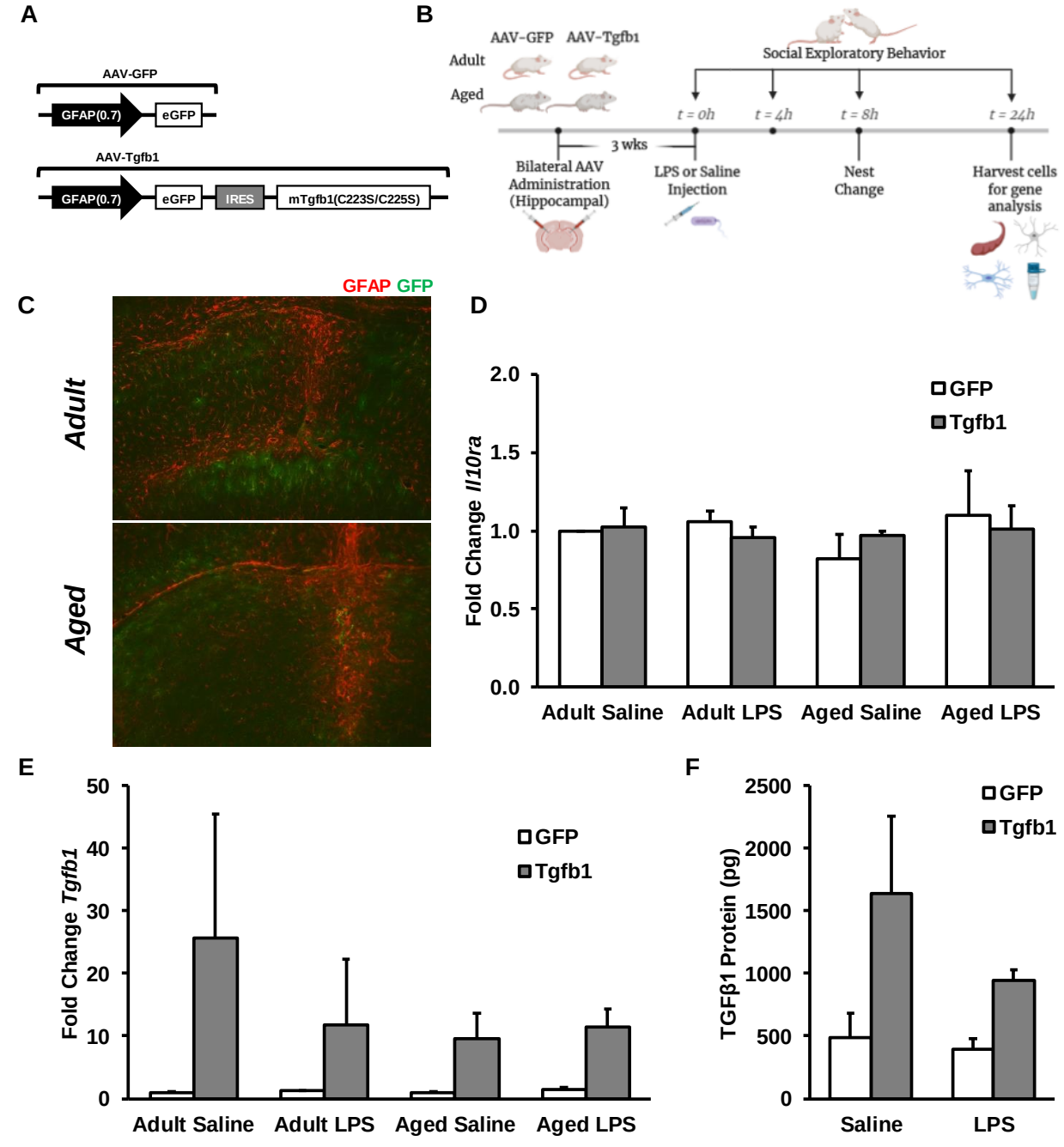
A
AAV-GFP
GFAP(0.7)
eGFP
AAV-Tgfb1
GFAP(0.7)
eGFP
IRES
mTgfb1(C223S/C225S)
B
AAV-GFP
AAV-Tgfb1
Adult
Aged
Social Exploratory Behavior
t = 0h
t = 4h
t = 8h
t = 24h
3 wks
Bilateral AAV Administration (Hippocampal)
LPS or Saline Injection
Nest Change
Harvest cells for gene analysis
C
GFAP GFP
Adult
Aged
D
Fold Change Il10ra
2.0
1.5
1.0
0.5
0.0
GFP
Tgfb1
Adult Saline
Adult LPS
Aged Saline
Aged LPS
E
Fold Change Tgfb1
50
40
30
20
10
0
GFP
Tgfb1
Adult Saline
Adult LPS
Aged Saline
Aged LPS
F
TGFβ1 Protein (pg)
2500
2000
1500
1000
500
0
GFP
Tgfb1
Saline
LPS

Figure 6

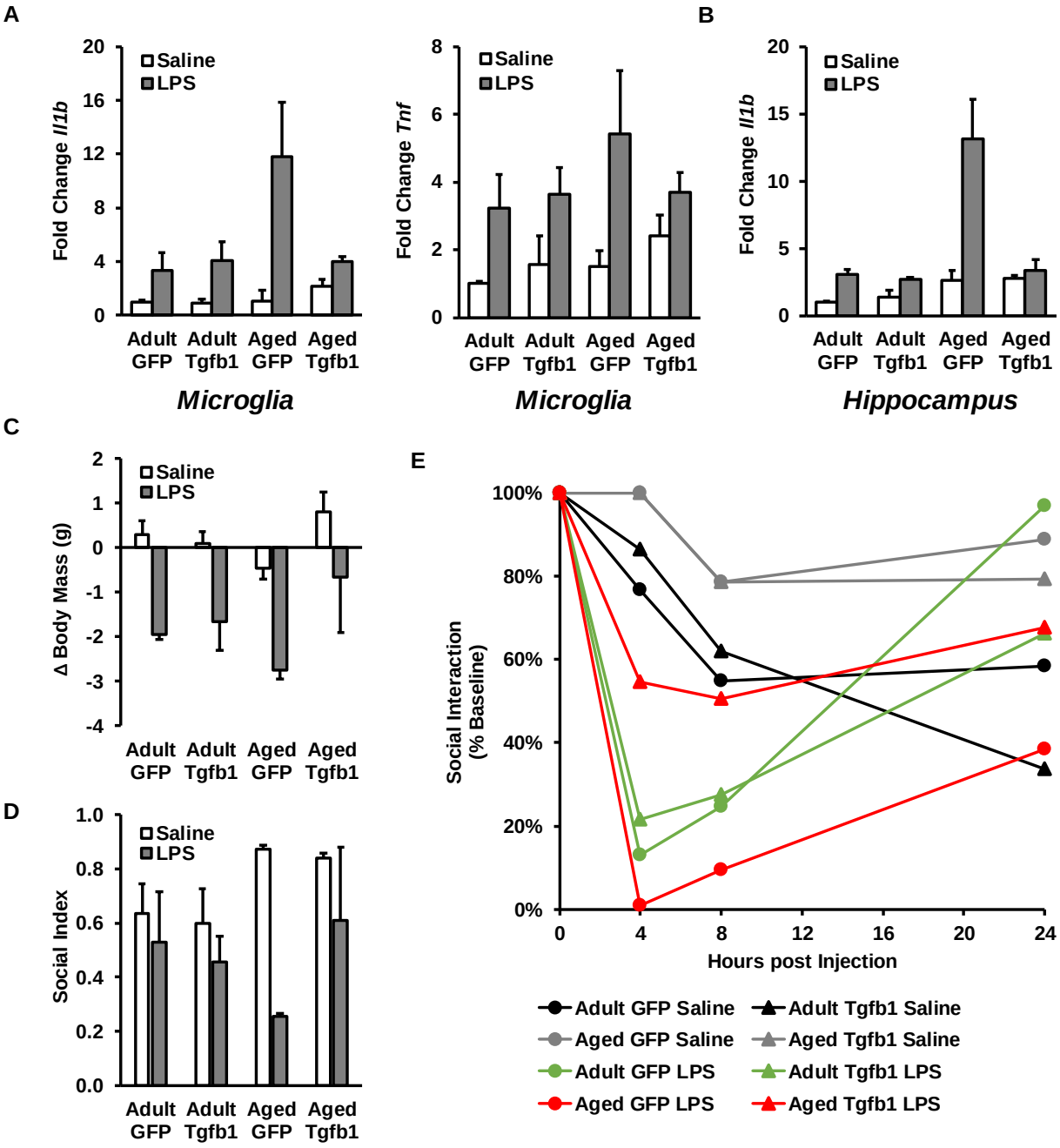
A
B
C
D
E
Saline
LPS
Fold Change Il1b
Fold Change Tnf
Fold Change Il1b
Adult GFP
Adult Tgfb1
Aged GFP
Aged Tgfb1
Microglia
Microglia
Hippocampus
Δ Body Mass (g)
Social Index
Social Interaction (% Baseline)
Hours post Injection
Adult GFP Saline
Adult Tgfb1 Saline
Aged GFP Saline
Aged Tgfb1 Saline
Adult GFP LPS
Adult Tgfb1 LPS
Aged GFP LPS
Aged Tgfb1 LPS

FIGURE LEGENDS

Figure 1. Astrocyte-specific *Il10ra* knockout impairs propagation of a functional TGFβ response. Cre/*lox* recombination was utilized to produce an IL-10Rα$^{A\text{-}cKO}$ line allowing for conditional, astrocyte-specific knockout of IL-10 receptor upon tamoxifen administration. (A) Aldh1l1-CreEr^{T2} mice were crossed with IL-10Rα^{flox} mice to 'flox' out Exon 3 of *Il10ra* and inhibit functionality of IL-10 protein. (B) Induction of tamoxifen and verification of Cre/*lox* recombination were confirmed with representative immunohistochemistry imaging of tdTomato reporter mice. (C) Adult (8 wks) Cre^{-} (control) and Cre^{+} (*Il10ra* knockout) mice were given intraperitoneal (i.p.) injections of saline or 0.50 mg/kg LPS (n = 9 mice/group) and processed for Percoll-enriched glial cells (as previously described) and representative brain slices 4 h and 24 h post-injection. Expression levels of *Il10ra* were analyzed from glial and brain tissue via qPCR at t = 24 h. (D) Expression levels of *Tgfb1* mRNA were measured by qPCR as fold change from a control group at t = 4 h and t = 24 h, respectively. Means with † denote $P < 0.05$ compared to the genotype-matched saline control group. Means with * denote $P < 0.05$ compared to the treatment-matched Cre^{-} group.

Figure 2. Impairment of TGFβ-mediated attenuation facilitates acute microglial activation and exaggerated sickness behavior 4 hours after peripheral immune challenge. (A) Male adults from the IL-10Rα$^{A\text{-}cKO}$ line (as previously described) and Cre^{-} controls were administered 1.5 mg i.p. tamoxifen in corn oil (10 mg/mL) daily for five days to induce *Il10ra* knockout. (B) Diagram of experimental design with t = 4 h endpoint. In brief, adult (8 wks) male Cre^{-} (control) and Cre+ (*Il10ra* KO) mice were given i.p. injections of saline or 0.50 mg/kg LPS (n = 9 mice/group) and sacrificed 4 h post-injection for harvesting and processing of coronal brain sections and Percoll-enriched glia. Social exploratory behavior was analyzed at t = 0 h and t = 4 h

post-injection. (C) As previously described, microglia were isolated from the 50/70 interface of a Percoll density gradient of brain tissue homogenate. mRNA was isolated from Percoll-enriched microglia using the RNeasy Mini Plus Kit and reversed transcribed to produce cDNA. qPCR was performed to analyze microglial gene expression of pro-inflammatory cytokines *Il1b* and *Tnf;* results were expressed as fold change from controls. (D) Representative 1-mm coronal brain sections were taken from each mouse and processed for mRNA through Tri-Reagent isolation protocol, followed by reverse transcription as previously described. Expression of reactive astrocyte marker *Gfap* was analyzed and expressed as fold change. (E) Diagram of social exploratory behavior paradigm. In brief, experimental subjects were allowed 5 minutes of open-field exploration, followed by introduction of a novel male juvenile mouse into their home cage for 5 additional minutes. Social investigation was assessed by duration of time spent investigating the novel mouse. (F) Social exploratory behavior was expressed as social interaction time at the t = 4 h timepoint normalized to baseline (t = 0 h) behavior activity. Means with † denote $P < 0.05$ compared to the genotype-matched saline control group. Means with * denote $P < 0.05$ compared to the treatment-matched Cre^- group.

Figure 3. Prolonged microglial neuroinflammation persists in an IL-10R$\alpha^{A\text{-}cKO}$ murine model 24 hours post-peripheral immune challenge. (A) Male adults from the IL-10R$\alpha^{A\text{-}cKO}$ line (previously described) and Cre^- controls were administered 1.5 mg i.p. tamoxifen in corn oil (10 mg/mL) daily for five days to induce *Il10ra* knockout. (B) Diagram of experimental design with t = 24 h endpoint. In brief, adult male Cre^- and Cre^+ were given i.p. injections of saline or 0.50 mg/kg LPS (n = 9 mice/group) and sacrificed 24 h post-injection. Coronal brain sections (1-mm, Bregma – 1.5 mm) were harvested, with remaining brain tissue homogenized and layered with

Percoll density gradients to isolate microglia. Social exploration behavior was recorded and analyzed at t = 0 h, 4 h, 8 h, and 24 h post-injection for interaction time and social index. Fresh nestlets were weighed and placed in home cages of test subjects at t = 0 h and weighed at t = 24 h to assess nesting behavior. Masses of test subjects and their food were recorded at t = 0 h and t = 24 h to assess sickness-associated weight and diet changes, respectively. (C) Percoll-enriched microglia were processed to produce cDNA, as previously described. qPCR was performed to analyze microglial gene expression of pro-inflammatory cytokines *Il1b* and *Tnf* and results were expressed as fold change from a control group. (D) mRNA was isolated from coronal brain sections with Tri-Reagent as previously described and reverse transcribed to prepare cDNA for qPCR analysis. Reactive astrocyte markers *Gfap* and *Vim* were analyzed as fold change from a control group to assess astrocyte reactivity in the brain microenvironment. Means with † denote $P < 0.05$ compared to the genotype-matched saline control group. Means with * denote $P < 0.05$ compared to the treatment-matched Cre^- group.

Figure 4. Unresolved knockout-mediated microglial activation and neuroinflammation underlies prolonged social withdrawal sickness behavior. (A) As previously described, body masses of test subjects were recorded 0 h and 24 h post-injection to assess sickness-associated weight changes. (B) Masses of standard rodent chow were recorded at t = 0 h and t = 24 h to assess sickness-associated differences in food consumption. (C) At t = 8 h, nests in each home cage were replaced with a fresh cotton nestlet. The mass of the nestlet was recorded at t = 8 h and t = 24 h to assess differences in nesting behavior as an indicator of prolonged sickness. (D) Social exploration behavior was assessed 0 h, 4 h, 8 h, and 24 h post-injection as previously described. Social index was calculated as normalized area under the curve of social interaction as a function of time, with

a higher value reflecting more time overall spent interacting with the introduced juvenile mouse. (E) A holistic time course of social interaction at each time point, normalized to baseline activity level. Means with † denote $P < 0.05$ compared to the genotype-matched saline control group. Means with * denote $P < 0.05$ compared to the treatment-matched Cre^- group.

Figure 5. Viral Tgfb1 administration circumvents IL-10 receptor insensitivity and augments TGFβ expression in aged mice. (A) Visual representation of the adeno-associated virus (AAV) vector for augmentation of TGFβ. Each vector was comprised of an AAV5 capsid and AAV2 ITR (AAV2/5 hybrid serotype). The experimental vector (AAV-TGFβ) expressed enhanced green fluorescent protein (eGFP) and *Tgfb1*; the control vector (AAV-GFP) expressed eGFP only. (B) Diagram of AAV2/5 experimental design. In brief, in a 2 x 2 x 2 factorial design, adult (6-8 wks) and aged (16-18 mo.) male BALB/c mice were administered AAV-GFP or AAV-TGFβ directly to the hippocampus (-1.82 mm AP, ±1.57 ML, +1.85 DV) in each hemisphere via stereotactic craniotomy and intra-cerebral injection (10^{10} GC per 2-μL). Three weeks thereafter, test subjects were given i.p. injections of 0.33 mg/kg LPS or saline (t = 0 h). As previously described, social exploratory behavior was recorded and analyzed at t = 0 h, 4 h, 8 h, and 24 h, with body masses recorded at t = 0 h and 24 h for weight change assessment. At t = 24 h, test subjects (n = 2 mice/group) were sacrificed and hippocampi from each hemisphere were micro-dissected and frozen in liquid nitrogen, with remaining brain tissue processed for Percoll-enrichment and isolation of glia, as previously described. (C) Adult and aged AAV-GFP mice were sacrificed and brains transcardially perfused with 5 mL ice-cold PBS and fixed with 5 mL 4% paraformaldehyde. Brains were flash-frozen, cryosectioned, and prepared for fluorescent histological analysis via immunohistochemistry (1°: GFAP, 1:500, Abcam; 2°: Alexa Fluor 594, 1:500, Invitrogen), and

imaged with EVOS Cell Imaging System fluorescence microscopy. (D) Astrocytes were isolated from the 35/50 interface of Percoll density gradient and processed for mRNA and cDNA. qPCR quantification of *Il10ra* mRNA was expressed as fold change from control group. (E) Hippocampal mRNA was isolated with Tri-Reagent protocol and reverse transcribed to cDNA for qPCR analysis. Expression level of *Tgfb1* was measured as fold change from control group. (F) Hippocampal tissue was sonicated in Tissue Protein Extraction Reagent and TGFβ protein concentrations were determined with ELISA Kit PicoKine^{TM} protocol and standardized for expression as mass (pg).

Figure 6. Augmentation of TGFβ ameliorates microglial activation and subsequent age-associated sickness behavior. Adult (6-8 wks) and aged (16-18 mo.) male BALB/c mice were administered AAV-TGFβ or AAV-GFP and 0.33 mg/kg LPS or saline, then sacrificed and processed at t = 24 h as previously described (n = 2 mice/group). (A) Percoll-enriched microglia were isolated from the 50/70 interface of a Percoll density gradient and processed with RNeasy Mini Plus kit to isolate mRNA. mRNA was reverse transcribed to produce cDNA for qPCR analysis. Pro-inflammatory microglial markers *Il1b* and *Tnf* were quantified and expressed as fold change from a control group. (B) Hippocampal cDNA was quantified by qPCR as previously described. Expression levels of *Il1b* was normalized as fold change from control group. (C) Body masses of test subjects were recorded at t = 0 h and 24 h and assessed for change (Δ) in body mass. (D) Social exploration behavior was recorded and analyzed at t = 0 h, 4 h, 8 h, and 24 h. Social index (SI) was calculated as normalized area under the curve of social interaction as a function of time, where higher SI values reflected higher social interaction levels. (E) A time course of social exploratory behavior by group over 24 h, normalized to baseline activity level.

ACKNOWLEDGEMENTS

I would like to begin by thanking Dr. Jonathan Godbout for the guidance, mentorship, and resources he has provided throughout my undergraduate education. From my first days as a freshman in the lab to the final touches on my senior thesis, his support has helped shaped the person and scientist I am today and thoroughly prepared me for lifelong learning in science and medicine. My intellectual and personal growth during my time in his lab have been profound. Dr. Godbout has established a culture of excellence in research, teaching, and compassion in our laboratory group, evident in the individual and group achievements of every student and associate of the lab. Beyond development of knowledge, critical thinking, and technical skills, I have forged lifelong friendships and relationships. All of this owes to Dr. Godbout's incredible mentorship and leadership abilities and reflect his passion for science and teaching.

Of course, no recollection of my research experience gets very far without mentioning doctoral candidate Shane O'Neil. I will forever be grateful for his willingness to take me under his wing and the outstanding mentorship that followed. I can't say enough about the impact Shane's guidance has had on my professional and personal life. His commitment to setting a strong foundation and patiently building skills cultivated the scientist I am today. Without his leadership by example and remarkable teaching acumen, this thesis would not be possible. Shane genuinely cares that we understand everything we are learning, and he goes above and beyond to support us. Perhaps most importantly, he is always there – there in times of need, there to answer questions, there to crack a witty joke. For these reasons and numerous others, I have no doubt that he will make an outstanding professor one day. Any student will be lucky to have his mentorship, something I will always appreciate dearly.

I would also like to thank all members of the Godbout lab for their various intellectual, bench, and social contributions to this project and my time in lab. I would like to thank fellow

mentees Emma Hans and Andrew Perl for their countless hours of behavior analysis, tissue processing, and intellectual contributions to this project. I am lucky to have worked with such bright and hardworking undergraduate peers and know great things lie ahead of them. A big thank you also goes to Chelsea Bray, Damon DiSabato, and Braedan Oliver for their assistance in tissue processing and AAV injections. Dr. Godbout and Shane O'Neil led project conceptualization, experimental design, and data analysis. I would like to recognize and express my gratitude for the support of my friends and colleagues in the Godbout, Kokiko-Cochran, and Sheridan labs and beyond. Finally, the support of my parents, Shanhe and Liping, and my brother and sister-in-law, Silis and Fernanda, mean the entire world to me. Their unconditional love and unwavering support have guided me through many ups and downs and provided me with everything I could have ever asked for.

This research was supported by an NIA R01 AG0151902-01 grant awarded to Dr. Jonathan Godbout by the National Institute on Aging. Additionally, Shane O'Neil is supported by the OSU CTOC T32 (NIDCR DE014320) training grant through The Ohio State University College of Dentistry and National Institute of Dental and Craniofacial Research.

REFERENCES

[1] W. He, D. Goodkind and P. Kowal, "An Aging World: 2015," United States Census Bureau, Washington, DC, 2016.

[2] P. D. Department of Economic and Social Affairs, "World Population Prospects 2019: Highlights," United Nations, New York, 2019.

[3] S. Johnny Lau, J.-F. Schlender, P. W. Slattum, D. L. Heald and R. O'Connor-Semmes, "Geriatrics 2030: Developing Drugs to Care for Older Persons - A Neglected and Growing Population," *Clinical Pharmacology & Therapeutics*, vol. 107, no. 1, pp. 53-56, 2020.

[4] A. W. Corona, A. M. Fenn and J. P. Godbout, "Cognitive and Behavioral Consequences of Impaired Immunoregulation in Aging," *Journal of Neuroimmune Pharmacology*, vol. 7, pp. 7-23, 2012.

[5] J. P. Godbout and R. W. Johnson, "Age and Neuroinflammation: A Lifetime of Psychoneuroimmune Consequences," *Neurologic Clinics*, vol. 24, no. 3, pp. 521-538, 2006.

[6] S. M. O'Neil, K. G. Witcher, D. B. McKim and J. P. Godbout, "Forced turnover of aged microglia induces an intermediate phenotype but does not rebalance CNS enivronmental cues driving priming to immune challenge," *Acta Neuropathologica Communications*, vol. 6, pp. 129-148, 2018.

[7] J. P. Godbout, J. Chen, A. F. Richwine, B. M. Berg, K. Kelley and R. W. Johnson, "Exaggerated neuroinflammation and sickness behavior in aged mice after activation of the peripheral innate immune system," *FASEB Journal*, vol. 19, no. 10, pp. 1329-31, 2005.

[8] C. E. Thomas, G. Schiedner, S. Kochanek, M. G. Castro and P. R. Lowenstein, "Peripheral infection with adenovirus causes unexpected long-term brain inflammation in animals injected intracranially with first-generation, but not with high-capacity, adenovirus vectors: Toward realistic long-term neurological gene therapy for chronic," *Proceedings of the National Academy of Sciences of the United States of America*, vol. 97, no. 13, pp. 7482-7487, 2000.

[9] K. Rockwood, S. Cosway, D. Carver, P. Jarrett, K. Stadnyk and J. Fisk, "The risk of dementia and death after delirium," *Age and Ageing*, vol. 28, pp. 551-556, 1999.

[10] T. J. Iwashyna, E. W. Ely, D. M. Smith and K. M. Langa, "Long-term Cognitive Impairment and Functional Disability Among Survivors of Severe Sepsis," *JAMA*, vol. 304, no. 16, pp. 1787-1794, 2010.

[11] N. Dunn, M. Mullee, H. V. Perry and C. Holmes, "Association between Dementia and Infectious Disease: Evidence from a Case-Control Study," *Alzhiemer Disease & Associated Disorders*, vol. 19, no. 2, pp. 91-94, 2005.

[12] C. J. Heyser, E. Masliah, A. Samimi, I. L. Campbell and L. H. Gold, "Progressive decline in avoidance learning paralleled by inflammatory neurodegeneration in transgenic mice expressing interleukin 6 in the brain," *Proceedings of the National Academy of Sciences of the United States of America*, vol. 94, pp. 1500-1505, 1997.

[13] Y. Hou, X. Dan, M. Babbar, Y. Wei, S. G. Hasslebalch, D. L. Croteau and V. A. Bohr, "Ageing as a risk factor for neurodegenerative disease," *Nature Reviews Neurology*, vol. 15, pp. 565-581, 2019.

[14] T. Wyss-Coray, "Ageing, neurodegeneration and brain rejuvenation," *Nature,* vol. 539, pp. 180-186, 2016.

[15] C. López-Otín, M. A. Blasco, L. S. M. Partridge and G. Kroemer, "The Hallmarks of Aging," *Cell,* vol. 153, no. 6, pp. 1194-1217, 2013.

[16] F. B. Garcez, D. Apolinario, F. Campora, J. A. E. Curiati, W. Jacob-Filho and T. J. Avelino-Silva, "Delirium and post-charge dementia: results from a cohort of older adults without baseline cognitive impairment," *Age and Ageing,* vol. 48, pp. 845-851, 2019.

[17] A. W. Corona, D. M. Norden, J. P. Skendelas, Y. Huang, J. C. O'Connor, M. Lawson, R. Dantzer, K. W. Kelley and J. P. Godbout, "Indoleamine 2,3-dioxygenase inhibition attenuates lipopolysaccharide induced persistent microglial activation and depressive-like complications in fractalkine receptor (CX3CR1)-deficient mice," *Brain, Behavior, and Immunity,* vol. 31, pp. 134-142, 2013.

[18] J. C. Jackson, S. M. Gordon, R. P. Hart, R. O. Hopkins and E. W. Ely, "The Association Between Delirium and Cognitive Decline: A Review of the Empirical Literature," *Neuropsychology Review,* vol. 14, no. 2, pp. 87-98, 2004.

[19] R. Dantzer, J. C. O'Connor, G. G. Freund, R. W. Johnson and K. W. Kelley, "From inflammation to sickness and depression: when the immune system subjugates the brain," *Nature Reviews Neuroscience,* vol. 9, pp. 46-57, 2008.

[20] D. M. Norden, P. J. Trojanowski, E. Villanueva, E. Navarro and J. P. Godbout, "Sequential Activation of Microglia and Astrocyte Cytokine Expression Precedes Increased Iba-1 or GFAP Immunoreactivity Following Systemic Immune Challenge," *Glia,* vol. 64, pp. 300-316, 2016.

[21] N. Quan and W. A. Banks, "Brain-immune communication pathways," *Brain, Behavior, and Immunity,* vol. 21, pp. 727-735, 2007.

[22] J. P. Godbout, M. Moreau, J. Lestage, J. Chen, N. L. Sparkman, J. O'Connor, N. Castanon, K. W. Kelley, R. Dantzer and R. W. Johnson, "Aging Exacerbates Depressive-like Behavior in Mice in Response to Activation of the Peripheral Innate Immune System," *Neuropsychopharmacology,* vol. 33, no. 10, pp. 2341-2351, 2008.

[23] R. Dantzer and K. W. Kelley, "Twenty years of research on cytokine-induced sickness behavior," *Brain, Behavior and Immunity,* vol. 21, pp. 153-160, 2007.

[24] C. J. Henry, Y. Huang, A. M. Wynne and J. P. Godbout, "Peripheral lipopolysaccharide (LPS) challenge promotes microglial hyperactivity in aged mice that is associated with exaggerated induction of both pro-inflammatory IL-1β and anti-inflammatory IL-10 cytokines," *Brain, Behavior, and Immunity,* vol. 23, pp. 309-317, 2009.

[25] J. P. Konsman, P. Parnet and R. Dantzer, "Cytokine-induced sickness behaviour: mechanisms and implications," *TRENDS in Neurosciences,* vol. 25, no. 3, pp. 154-159, 2002.

[26] B. M. Berg, J. P. Godbout, K. W. Kelley and R. W. Johnson, "α-Tocopherol attenuates lipopolysaccharide-induced sickness behavior in mice," *Brain, Behavior, and Immunity,* vol. 18, pp. 149-157, 2004.

[27] R. M. Barrientos, L. R. Watkins, J. W. Rudy and S. F. Maier, "Characterization of the sickness response in young and aging rats following E. coli infection," *Brain, Behavior, and Immunity,* vol. 23, pp. 450-454, 2009.

[28] D. M. Norden, M. M. Muccigrosso and J. P. Godbout, "Microglial priming and enhanced reactivity to secondary insult in aging, and traumatic CNS injury, and neurodegenerative disease," *Neuropharmacology,* vol. 96, no. A, pp. 29-41, 2015.

[29] R. M. Ransohoff and V. H. Perry, "Microglial Physiology: Unique Stimuli, Specialized Responses," *Annual Review of Immunology,* vol. 27, pp. 119-145, 2009.

[30] S. M. Matt and R. W. Johnson, "Neuro-immune dysfunction during brain aging: new insights in microglial cell regulation," *Current Opinion in Pharmacology,* vol. 26, pp. 96-101, 2016.

[31] R. N. Dilger and R. W. Johnson, "Aging, microglial cell priming, and the discordant central inflammatory response to signals from the peripheral immune system," *Journal of Leukocyte Biology,* vol. 84, pp. 932-939, 2008.

[32] D. M. Norden, A. M. Fenn, A. Dugan and J. P. Godbout, "TGFβ Produced by IL-10 Redirected Astrocytes Attenuates Microglial Activation," *Glia,* vol. 62, pp. 881-895, 2014.

[33] R. Verma, L. Balakrishnan, K. Sharma, A. A. Khan, J. Advani, H. Gowda, S. P. Tripathy, M. Suar, A. Pandey, S. Gandotra, T. K. Prasad and S. Shankar, "A network map of Interleukin-10 signaling pathway," *Journal of Cell Communication and Signaling,* vol. 10, pp. 61-67, 2016.

[34] A. M. Wynne, C. J. Henry, Y. Huang, A. Cleland and J. P. Godbout, "Protracted downregulation of CX3CR1 on microglia of aged mice after lipopolysaccharide challenge," *Brain, Behavior, and Immunity,* vol. 24, pp. 1190-1201, 2010.

[35] A. Suzumura, M. Sawada, H. Yamamoto and T. Marunouchi, "Transforming Growth Factor-beta Suppresses Activation and Proliferation of Microglia in Vitro," *The Journal of Immunology,* vol. 151, pp. 2150-2158, 1993.

[36] O. Butovsky, M. P. Jedrychowski, C. S. Moore, R. Cialic, A. J. Lanser, G. Gabriely, T. Koeglsperger, B. Dake, P. M. Wu, C. E. Doykan, Z. Fanek, L. Liu, Z. Chen, J. D. Rothstein, R. M. Ransohoff, S. P. Gygi, J. P. Antel and H. L. Weiner, "Identification of a unique TGF-β-dependent molecular and functional signature in microglia," *Nature Neuroscience,* vol. 17, no. 1, pp. 131-143, 2013.

[37] D. M. Norden, P. J. Trojanowski, F. R. Walker and J. P. Godbout, "Insensitivity of astrocytes to interleukin 10 signaling following peripheral immune challenge results in prolonged microglial activation in the brain," *Neurobiology of Aging,* vol. 44, pp. 22-41, 2016.

[38] A. P. Hutchins, D. Diez and D. Miranda-Saavedra, "The IL-10/STAT3-mediated anti-inflammatory response: recent developments and future challenges," *Briefings in Functional Genomics,* vol. 12, no. 6, pp. 489-498, 2013.

[39] E. S. Wohleb, A. M. Fenn, A. M. Pacenta, N. D. Powell, J. F. Sheridan and J. P. Godbout, "Peripheral innate immune challenge exaggerated microglia activation, increased the number of inflammatory CNS macrophages, and prolonged social withdrawal in socially defeated mice," *Psychoneuroendocrinology,* vol. 37, pp. 1491-1505, 2012.

[40] P. Chakrabarty, A. Rosario, P. Cruz, Z. Siemienski, C. Ceballos-Diaz, K. Crosby, K. Jansen, D. R. Borchelt, J.-Y. Kim, J. L. Jankowsky, T. E. Golde and Y. Levites, "Capsid Serotype and Timing of Injection Determines AAV Transduction in the Neonatal Mice Brain," *Plos One,* vol. 8, no. 6, pp. 1-9, 2013.

[41] J. Winchenbach, T. Düking, S. A. Berghoff, S. K. Stumpf, S. Hülsmann, K.-A. Nave and G. Saher, "Inducible targeting of CNS astrocytes in Aldh1l1-CreERT BAC transgenic mice," *F1000Research,* vol. 5, p. 2934, 2016.

[42] H. Yoon, G. Walters, A. R. Paulsen and I. A. Scarisbrick, "Astrocyte heterogeneity across the brain and spinal cord occurs developmentally, in adulthood and in response to demyelination," *PLOS ONE,* vol. 12, no. 7, pp. 1-19, 2017.

[43] E. M. Hol and M. Pekny, "Glial fibrillary acidic protein (GFAP) and the astrocyte intermediate filament system in diseases of the central nervous system," *Current Opinion in Cell Biology,* vol. 32, pp. 121-130, 2015.

[44] D. G. Diniz, M. Augusto de Oliveira, C. Mendes de Lima, C. A. R. Fôro, M. C. K. Sosthenes, J. Bento-Torres, P. F. d. Vasconcelos, D. C. Anthony and C. W. P. Diniz, "Age, environment, object recognition and morphological diversity of GFAP-immunolabeled astrocytes," *Behavioral and Brain Functions,* vol. 12, no. 28, pp. 1-19, 2016.

[45] M. Soffié, K. Hahn, E. Terao and F. Eclancher, "Behavioural and glial changes in old rats following environmental enrichment," *Behavioural Brain Research,* vol. 101, pp. 37-49, 1999.

[46] M. Pekny, W. Ulrika, T. Tatlisumak and M. Pekna, "Astrocyte activation and reactive gliosis - A new target in stroke?," *Neuroscience Letters,* vol. 689, pp. 45-55, 2019.

[47] M. Pekny and M. Pekna, "Astrocyte Reactivity and Reactive Astrogliosis: Costs and Benefits," *Physiological Reviews,* vol. 94, pp. 1077-1098, 2014.

[48] J. E. Eriksson, T. Dechat, B. Grin, B. Helfand, M. Mendez, H.-M. Pallari and R. D. Goldman, "Introducing intermediate filaments: from discovery to disease," *The Journal of Clinical Investigation,* vol. 119, no. 7, pp. 1763-1771, 2009.

[49] Y.-B. Lu, I. Iandiev, M. Hollborn, N. Körber, E. Ulbricht, P. G. Hirrlinger, T. Pannicke, E.-Q. Wei, A. Bringmann, H. Wolburg, U. Wilhelmmson, M. Pekny, P. Wiedemann, A. Reichenbach and J. A. Käs, "Reactive glial cells: increased stiffness correlates with increased intermediate filament expression," *The FASEB Journal,* vol. 25, pp. 624-631, 2011.

[50] K. Sugaya, M. Chouinard, R. Greene, M. Robbins, D. Personett, C. Kent, M. Gallagher and M. McKinney, "Moelcular Indices of Neuronal and Glial Plasticity in the Hippocampal Formation in a Rodent Model of Age-Induced Spatial Learning Impairment," *The Journal of Neuroscience,* vol. 16, no. 10, pp. 3427-3443, 1996.

[51] A. Haque, J. Engel, S. A. Teichmann and T. Lönnberg, "A practical guide to single-cell RNA-sequencing for biomedical research and clinical applications," *Genome Medicine,* vol. 9, no. 75, pp. 1-12, 2017.

[52] D. R. Seals and S. Melov, "Translational Geroscience: Emphasizing function to achieve optimal longevity," *Aging,* vol. 6, no. 9, pp. 718-730, 2014.